THE JOURNAL OF BIOLOGICAL CHEMISTRY
Vol. 273, No. 17, Issue of April 24, pp. 10279–10287, 1998

Printed in U.S.A.

Molecular Cloning and Functional Characterization of a Novel Receptor-activated TRP Ca^{2+} Channel from Mouse Brain*

(Received for publication, November 4, 1997, and in revised from, January 28, 1998)

Takaharu Okada‡, Shunichi Shimizu‡, Minoru Wakamori‡, Akito Maeda¶, Tomohiro Kurosaki¶, Naoyuki Takada‡§, Keiji Imoto‡, and Yasuo Mori‡§‖

From the ‡Department of Information Physiology, National Institute for Physiological Sciences, Okazaki 444, Japan, the §Institute of Molecular Pharmacology and Biophysics, University of Cincinnati College of Medicine, Cincinnati, Ohio 45267-0828, and the ¶Department of Molecular Genetics, Institute for Liver Research, Kansai Medical University, Moriguchi 570, Japan

Characterization of mammalian homologues of *Drosophila* TRP proteins, which induce light-activated Ca^{2+} conductance in photoreceptors, has been an important clue to understand molecular mechanisms underlying receptor-activated Ca^{2+} influx in vertebrate cells. We have here isolated cDNA that encodes a novel TRP homologue, TRP5, predominantly expressed in the brain. Recombinant expression of the TRP5 cDNA in human embryonic kidney cells dramatically potentiated extracellular Ca^{2+}-dependent rises of intracellular Ca^{2+} concentration ($[Ca^{2+}]_i$) evoked by ATP. These $[Ca^{2+}]_i$ transients were inhibited by SK&F96365, a blocker of receptor-activated Ca^{2+} entry, and by La^{3+}. Expression of the TRP5 cDNA, however, did not significantly affect $[Ca^{2+}]_i$ transients induced by thapsigargin, an inhibitor of endoplasmic reticulum Ca^{2+}-ATPases. ATP stimulation of TRP5-transfected cells pretreated with thapsigargin to deplete internal Ca^{2+} stores caused intact extracellular Ca^{2+}-dependent $[Ca^{2+}]_i$ transients, whereas ATP suppressed $[Ca^{2+}]_i$ in thapsigargin-pretreated control cells. Furthermore, in ATP-stimulated, TRP5-expressing cells, there was no significant correlation between Ca^{2+} release from the internal Ca^{2+} store and influx of extracellular Ca^{2+}. Whole-cell mode of patch-clamp recording from TRP5-expressing cells demonstrated that ATP application induced a large inward current in the presence of extracellular Ca^{2+}. Omission of Ca^{2+} from intrapipette solution abolished the current in TRP5-expressing cells, whereas 10 nM intrapipette Ca^{2+} was sufficient to support TRP5 activity triggered by ATP receptor stimulation. Permeability ratios estimated from the zero-current potentials of this current were $P_{Ca}:P_{Na}:P_{Cs}$ = 14.3:1.5:1. Our findings suggest that TRP5 directs the formation of a Ca^{2+}-selective ion channel activated by receptor stimulation through a pathway that involves Ca^{2+} but not depletion of Ca^{2+} store in mammalian cells.

Calcium (Ca^{2+}) influx across the plasma membrane plays a vital role in the regulation of diverse cellular processes, ranging from ubiquitous activities like gene expression to tissue-specific functions such as neurotransmitter release and muscle contraction, by controlling the cytosolic free Ca^{2+} concentration ($[Ca^{2+}]_i$) (1, 2). Recently, in addition to the well characterized modes of Ca^{2+} entry through voltage-dependent Ca^{2+} channels and ligand-gated cation channels, receptor-activated Ca^{2+} influx that occurs as a second phase of phosphatidylinositol (PI)[1]-dependent response, has been recognized for its physiological significance (3). Diverse ion channels activated by various triggers have been recognized to be responsible for the receptor-activated Ca^{2+} influx (3). Among members of the group, recent attention was particularly directed to capacitative Ca^{2+} entry (CCE; in other words, Ca^{2+} release-activated current (I_{CRAC}), or store-operated channel), that is activated through Ca^{2+} release from the intracellular Ca^{2+} store, endoplasmic reticulum (ER), induced by inositol 1,4,5-trisphosphate (IP_3) and consequent depletion of Ca^{2+} from the store (2–9). Diffusible small molecules (10, 11), IP_3 metabolites (12), and direct coupling of IP_3 receptors or small GTP-binding (G) proteins with the channel proteins (5, 6, 9) have been proposed to be involved in the activation of this Ca^{2+} entry pathway. Other plasma membrane ion channels directly activated by second messengers such as Ca^{2+}, IP_3, and inositol 1,3,4,5-tetraphosphate (IP_4) (13–16) are also categorized as receptor-activated Ca^{2+} channels (3).

An important clue for understanding the molecular basis of receptor-activated Ca^{2+} influx was first attained through the finding of a *Drosophila* visual transduction mutation *transient receptor potential* (*trp*), whose photoreceptors fail to generate the Ca^{2+}-dependent sustained phase of receptor potential and to induce subsequent Ca^{2+}-dependent adaptation to light (17, 18). Inasmuch as the gene products of the *trp* and *trp-like* (*trpl*) gene (TRP and TRPL) comprise the light-activated, PI-dependent Ca^{2+} conductance in *Drosophila* photoreceptors (19), the original hypothesis that the counterparts of TRP and TRPL are responsible for CCE in vertebrate cells was based upon analogy between the phototransduction mechanism in *Drosophila* and the PI-dependent signal transduction processes in vertebrates (18). In fact, recent molecular characterization has unveiled the existence of multiple genes encoding TRP homologues in vertebrate cells (20–25), and cDNA expression experiments of

* This work was supported by research grants from the Ministry of Education, Science, Sports, and Culture, the Japan Society for the Promotion of Science, and the Mochida Memorial Foundation for Promotion of Medicine and Pharmacy. The costs of publication of this article were defrayed in part by the payment of page charges. This article must therefore be hereby marked "*advertisement*" in accordance with 18 U.S.C. Section 1734 solely to indicate this fact.

The nucleotide sequence(s) reported in this paper has been submitted to the GenBank™/EBI Data Bank with accession number(s) AF029983.

‖ To whom correspondence should be addressed: Dept. of Information Physiology, National Institute for Physiological Sciences, Okazaki 444, Japan Tel.: 81-564-55-7855; Fax: 81-564-55-7853; E-mail: moriy@nips.ac.jp.

[1] The abbreviations used are: PI, phosphatidylinositol; IP_3, inositol 1,4,5-trisphosphate; IP_4, inositol 1,3,4,5-tetraphosphate; CCE, capacitative Ca^{2+} entry; I_{CRAC}, Ca^{2+} release-activated current; ER, endoplasmic reticulum; PCR, polymerase chain reaction; kb, kilobase pair(s); RT, reverse transcriptase; HEK, human embryonic kidney; HBS, HEPES-buffered saline.

TRP proteins present some lines of supportive evidence for the hypothesis that TRP and its homologues except TRPL are CCE channels (20, 23–31). However, the hypothesis is still controversial (19, 32, 33). Acharya *et al.* (33) demonstrated that photoreceptors from *Drosophila* with homozygous loss-of-function mutation of IP_3 receptors were indistinguishable from wild-type controls in sensitivity, kinetics, and adaptation of response to light. Furthermore, most significantly, low IP_3 concentrations can induce substantial Ca^{2+} release from the stores without activating Ca^{2+} entry at all in rat leukemia cells, suggesting that even the activation of CCE is not that tightly coupled to Ca^{2+} release from the IP_3-sensitive stores (12).

Thus, criteria of activation trigger, other than depletion of Ca^{2+} store, should be considered in functionally establishing cloned TRP channels to be correlated with native Ca^{2+} channels responsible for receptor-activated Ca^{2+} influx, including CCE.

We have here isolated cDNA that encodes a novel TRP homologue, TRP5, predominantly expressed in the brain. The recombinant expression of the TRP5 cDNA in human embryonic kidney (HEK) cells potentiated an extracellular Ca^{2+}-dependent increase of $[Ca^{2+}]_i$ evoked by ATP, but not by an inhibitor of ER Ca^{2+}-ATPases, thapsigargin. Whole-cell mode of patch-clamp recordings from TRP5-expressing cells demonstrated that ATP application induced a large inward current in the presence of extracellular Ca^{2+}, which reversed at a positive potential. Our findings suggest that TRP5 directs the formation of a highly Ca^{2+}-permeable ion channel that can be activated through receptor-operative pathways other than depletion of Ca^{2+} from Ca^{2+} stores in brain neurons.

EXPERIMENTAL PROCEDURES

cDNA Cloning and Sequence Determination—A mixture of oligo(dT)-primed cDNAs synthesized from the mouse (BALB/c or 129/SvJ) brain poly(A)$^+$ RNA was subjected to PCR amplification using a Marathon cDNA amplification kit (CLONTECH). Degenerate oligonucleotide primers used were 5′-TGGGGCC(T/C/A)(T/C)TGCAGAT(A/C)TC(T/A)-CTGGGA-3′ and 5′-(G/T)G(A/T)TCG(A/G)GCAAA(C/T)TTCCA(C/T)TC-3′. Obtained PCR products were subsequently subcloned into the T/A cloning plasmid, pCRII (Invitrogen, Carlsbad, CA), to yield pTRP15. Sequence comparison with a PCR product amplified using a pair of specific oligonucleotide primers T5–1 (5′-TATCTACTGCCTAGTACTA-CTGG-3′) and T5–2 (5′-GCAATGAGCTGGTAGGAGTTATTC-3′) according to the partial genomic nucleotide sequence given in Zhu *et al.* (24) confirmed that the cDNA insert carried by pTRP15 encodes mouse TRP5. Further screening was performed to obtain entire coding cDNAs for mouse TRP5. Oligo(dT)-primed, size-selected (>1 kilobase pairs (kb)) cDNA libraries constructed in the λ Uni-ZAP XR vector (Stratagene, La Jolla, CA) using poly(A)$^+$ RNA from the brain of adult BALB/c or postnatal 14-day-old (P14) C57BL/6J mice were screened to yield mouse TRP5 clones λm37 (1020–3166; nucleotide numbers from the first residue of the initiation ATG triplet) and λO4 (1134–3287 followed by a poly(dA) tract). Additional clones harboring cDNAs for the further upstream regions of mouse TRP5 were isolated by screening a specific oligonucleotide-primed cDNA transcripts of poly(A)$^+$ RNA from the brain of P14 C57BL/6J mice constructed in the λ Uni-ZAP XR vector. The specific oligonucleotide primer (5′-GAGAGAGAGAGAGAGAGAG-AACTAGTCTCGAGTCAAGCAGCATTCGTCCC-3′) was according to the sequence in the clone λm37 and was designed to contain an additional sequence of a *Xho*I site protected by GA repeats for subcloning into the λ Uni-ZAP XR vector. λO15 (−232 to 1547) and the other 13 hybridization-positive clones were isolated through hybridization with the 657-base pair *Eco*RI(on vector)/*Bam*HI(1665) fragment from λm37. cDNA clones were sequenced on both strands using an automated sequencer (model 373S; Perkin Elmer).

Northern Blot Analysis—RNA blot hybridization analysis was carried out using 20 μg of total RNA from various tissues. The probe was the ~0.9-kb *Eco*RI(on vector)/*Hin*dIII(2092) fragment from λm37. A random primer DNA labeling kit (version 2; Takara, Otsu, Japan) was used to prepare the ^{32}P-labeled probe. Hybridization was performed at 42 °C in 50% formamide, 5× SSC, 50 mM sodium phosphate buffer (pH 7.0), 0.1% SDS, 0.1% polyvinylpyrrolidone, 0.1% Ficoll 400 (Amersham Pharmacia Biotech), 0.1% bovine serum albumin, and 0.2 mg/ml sonicated herring sperm DNA, as described previously (34).

Reverse Transcriptase (RT)-PCR Amplification and Southern Blot Analysis—Reverse transcription and PCR amplification from 1 μg of total RNA were performed using r*Tth* DNA polymerase (RT-PCR high Plus; Toyobo, Osaka, Japan). Pairs of primers used for amplification of TRP5 and cyclophilin were T5–1 and T5–2 (see above), and 5′-GCAG-CCATGGTCAACCCCACCG-3′ and 5′-GAAATTAGAGCTGTCCACAG-TCGG-3′ (GenBank™ accession no. X52803), respectively. The thermocycler was programmed to give an initial cycle consisting of 60 °C reverse transcription for 5 min and 94 °C denaturation for 2 min, followed by 40 cycles of 94 °C denaturation for 1 min and 52 °C annealing/extension for 1.5 min. The final cycle was followed by an additional extension at 52 °C for 7 min. To verify the identity of the PCR products, Southern blots were hybridized with ^{32}P-5′-end-labeled synthetic oligonucleotide probes 5′-ATGAACCTAACAACTGCAAGG-3′ and 5′-CGA-CATCACGGCCGATGACGAGCCC-3′ for detection of TRP5 and cyclophilin mRNA, respectively. Hybridization was performed at 50 °C in 6× SSC, 50 mM sodium phosphate buffer (pH 7.0), 0.2% SDS, 0.1% polyvinylpyrrolidone, 0.1% Ficoll 400, 0.1% bovine serum albumin, and 0.1 mg/ml sonicated herring sperm DNA.

Recombinant Expression in HEK Cells—A PCR product amplified from the clone λO15 using a sense primer (5′-GGGTCGACGGGTTTT-TATTTTTAATTTTCTTTCAAATACTTCCACCATGGCCCAGCTGTAC-TAC-3′), designed to contain the untranslated leader sequence from the alfalfa mosaic virus (35), a consensus sequence for translation initiation (36), and nucleotide residues 1–18 of TRP5, and an antisense primer (5′-CCAAAGGATCCATGCAGTTGATGTTGAC-3′), was digested with *Sal*I and *Bam*HI. Another PCR product amplified from λO4 using a sense primer (5′-CCTCTGCAGATCTCTTTGGGACGAATGC-3′) and an antisense primer (5′-ATGGCGGCCGCAAAACATGAAGAATGTGGC-3′) was digested with *Pst*I and *Not*I. The resulting fragments were ligated with the *Bam*HI(199)/*Pst*I(1521) fragment from λO15 and the 5.5-kb *Sal*I/*Not*I fragment from pCI-neo (Promega, Madison, WI) to yield pCI-neo-mTRP5. HEK293 cells (RIKEN Cell Bank, Tsukuba, Japan) were transfected with the recombinant plasmids pCI-neo-mTRP5 plus πH3-CD8 containing the cDNA of the T-cell antigen CD8 (37). Transfection was carried out using SuperFect Transfection Reagent (QIAGEN, Hilden, Germany). Cells were trypsinized, diluted with Dulbecco's modified Eagle's medium containing 10% fetal bovine serum, 30 units/ml penicillin, and 30 μg/ml streptomycin, and plated onto glass coverslips 18 h after transfection. Then cells were subjected to measurements 36–66 h after plating on the coverslips. TRP5-expressing cells were selected through detection of CD8 coexpression using polystyrene microspheres precoated with antibody to CD8 (Dynabeads M-450 CD8; Dynal, Oslo, Norway).

Measurement of Changes in $[Ca^{2+}]_i$—Cells on coverslips were loaded with fura-2 by incubation in Dulbecco's modified Eagle's medium containing 5 μM fura-2/AM (Dojindo Laboratories, Kumamoto, Japan) and 10% fetal bovine serum at 37 °C for 30 min, and washed with HEPES-buffered saline (HBS) containing (in mM): 107 NaCl, 6 KCl, 1.2 $MgSO_4$, 2 $CaCl_2$, 1.2 KH_2PO_4, 11.5 glucose, 20 HEPES, adjusted to pH 7.4 with NaOH. The coverslips were then placed in a perfusion chamber mounted on the stage of the microscope. Fluorescence images of the cells were recorded and analyzed with a video image analysis system (ARGUS-50/CA, Hamamatsu Photonics, Hamamatsu, Japan) according to the method of Hazama and Okada (38). The fura-2 fluorescence at an emission wavelength of 510 nm (bandwidth, 20 nm) was observed at room temperature by exciting fura-2 alternately at 340 and 380 nm (bandwidth, 11 nm). The 340/380 nm ratio images were obtained on a pixel by pixel basis, and were converted to Ca^{2+} concentrations by *in vitro* calibration. The calibration procedure was performed according to Ueda and Okada (39). ATP (100 mM in water), SK&F96365 (10 mM in water), and thapsigargin (2 mM in dimethyl sulfoxide) were diluted to their final concentrations in HBS or Ca^{2+}-free HBS containing (in mM): 107 NaCl, 6 KCl, 1.2 $MgSO_4$, 1.2 KH_2PO_4, 0.5 EGTA, 11.5 glucose, 20 HEPES, adjusted to pH 7.4 with NaOH, and applied to the cells by perfusion. $LaCl_3$ and $GdCl_3$ (100 mM in water) were diluted in HBS or Ca^{2+}-free HBS from which KH_2PO_4 was omitted. The number of CD8-positive cells ranged from 2 to 8 in the field of view during an experiment. Data were accumulated under each condition from two to four experiments using cells prepared through two to three transfections.

Electrophysiology—For electrophysiological measurements, coverslips with cells were placed in dishes containing the solutions. Cells prepared in this manner had membrane capacitance of 21.3 ± 2.3 picofarads (n = 25). Currents from cells were recorded at room temperature using patch-clamp techniques of whole-cell mode (40) with an EPC-7 patch-clamp amplifier (List-Medical, Darmstadt, Germany).

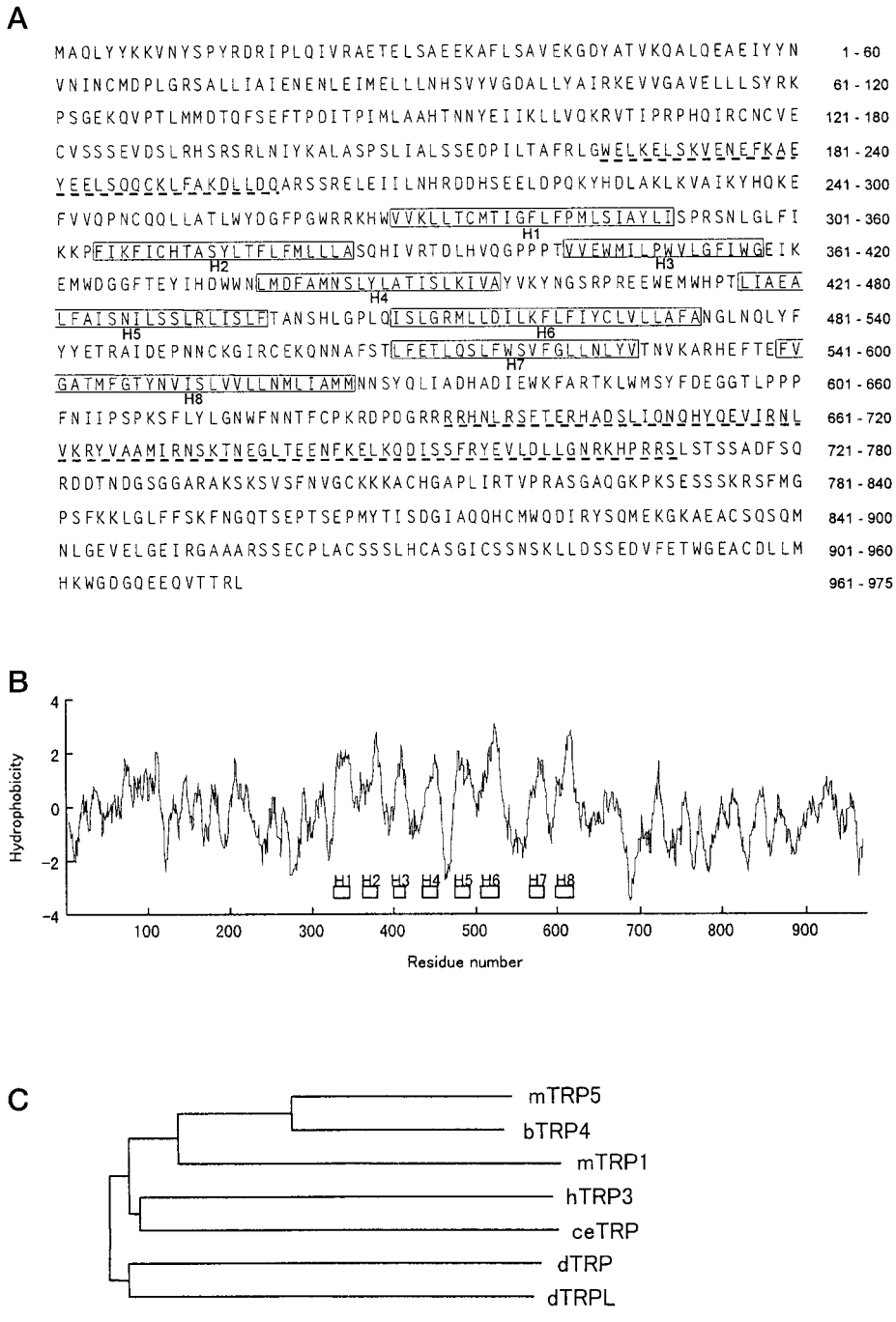

FIG. 1. **Primary structure and hydropathy analysis of TRP5, and phylogenetic tree of the TRP family.** In *A*, the amino acid sequence (in *single-letter code*) of the mouse brain TRP5 deduced from the cDNA sequence is shown. The hydrophobic regions H1–H8 are enclosed with *solid lines*. The domains predicted to form coiled-coil structure are *underlined* with *dashed lines*. In *B*, the Kyte-Doolittle hydrophobicity profile of TRP5 was generated with a window size of 10 amino acids (66). In *C*, the phylogenetic tree for the TRP family was generated using the Clustalw program (46). Members of the TRP family are as follows: dTRP (42), dTRPL (43), hTRP3 (24), bTRP4 (25), ceTRP (67), and mTRP1 (68).

Patch pipettes were made from borosilicate glass capillaries (1.5 mm, outer diameter; Hilgenberg, Malsfeld, Germany) using a model P-87 Flaming-Brown micropipette puller (Sutter Instrument, San Rafael, CA). Pipette resistance ranged from 2 to 4 megohms when filled with the pipette solution described below. Currents were sampled at 200 Hz after low-pass filtered at 1 kHz (−3 dB) using an 8-pole Bessle filter (900, Frequency Devices, Haverhill, MA) for Fig. 7 (*A* and *B*), sampled at 1 kHz for Fig. 7*C*, and analyzed with pCLAMP 6.02 software (Axon Instruments, Foster City, CA). The pipette solution for Fig. 7 contained (in mM): CsOH 105, aspartic acid 105, CsCl 40, $MgCl_2$ 2, $CaCl_2$ 3.2, EGTA 5, Na_2ATP 2, HEPES 5, adjusted to pH 7.2 with CsOH. Calculated free Ca^{2+} concentration was 200 nM. $CaCl_2$ was 1.33 and 0.34 mM in the pipette solution containing calculated free Ca^{2+} concentration of 50 and 10 nM, respectively. The "0Ca^{2+}" external solution contained (in mM): NaCl 140, $MgCl_2$ 1.2, $CaCl_2$ 1.2, EGTA 10, glucose 10, HEPES 11.5, adjusted to pH 7.4 with NaOH (8 nM calculated free Ca^{2+}). The "10Ca^{2+}" external solution contained (in mM): NaCl 122.4, $MgCl_2$ 1.2, $CaCl_2$ 10, glucose 30, HEPES 11.5, adjusted to pH 7.4 with NaOH. The osmolarity of the external solutions was adjusted to about 325 mOsM. Rapid exchange of the external solutions was made by a modified "Y-tube" method (41).

RESULTS

Primary Structure of TRP5—Fig. 1*A* shows the amino acid sequence of the mouse TRP5 deduced from the open reading frame of the corresponding cDNA sequence. The translation initiation codon is assigned to the first in-frame methionine codon downstream of a stop codon. TRP5 is composed of 975 amino acid residues with a hydropathy profile revealing eight hydrophobic segments and hydrophilic N and C termini (Fig. 1*B*), similar to those of other TRP subtypes (21, 22, 24, 25, 42, 43). Sufficient length of hydrophobic regions to span the membrane, together with the lack of a hydrophobic N-terminal sequence indicative of the signal sequence, suggests that TRP5 is a membrane protein with a core of transmembrane segments and the flanking N- and C-terminal regions disposed on the

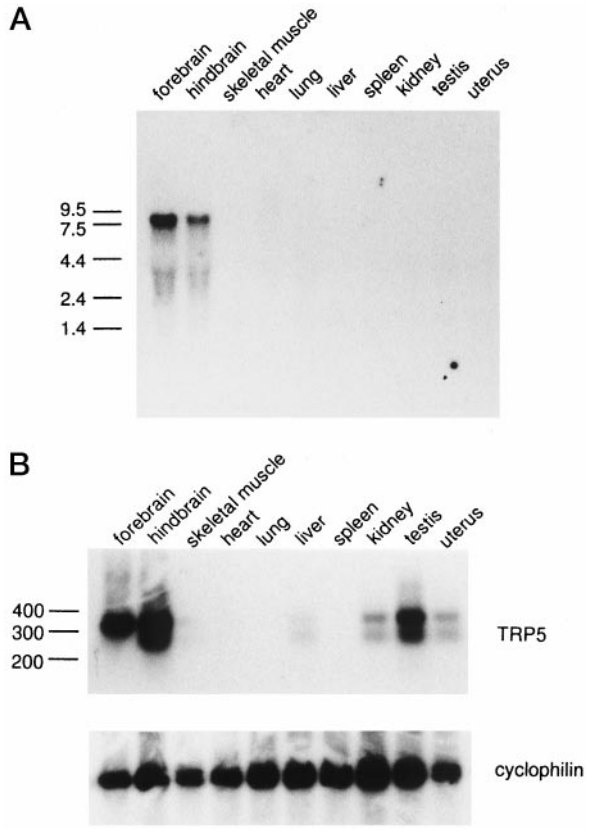

FIG. 2. **Distribution of TRP5 mRNA expression in the mouse tissues.** *A*, autoradiogram of blot hybridization analysis with a TRP5 cDNA probe of RNA from different tissues of mice. The positions and sizes (in kb) of the RNA markers are shown on the *left*. *B*, autoradiogram of blot hybridization analyses of TRP5 and cyclophilin cDNA fragments amplified by RT-PCR. Probes are 5′-end-labeled oligonucleotides internal to the primers used for PCR. The positions and sizes (in base pairs) of DNA markers are shown on the *left*.

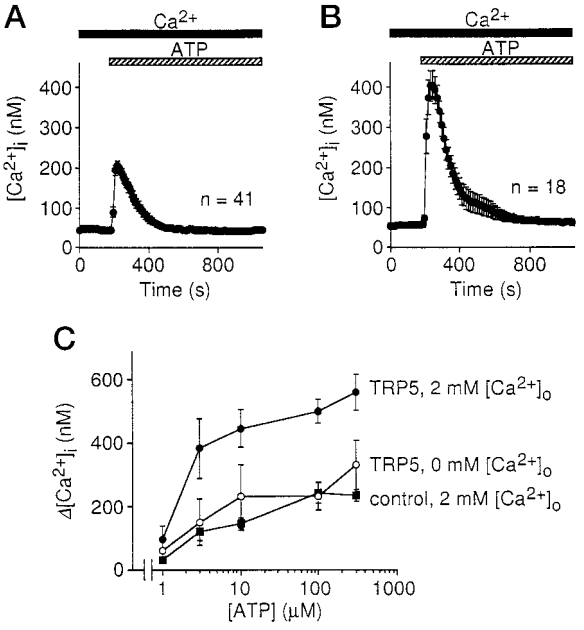

FIG. 3. **ATP-induced $[Ca^{2+}]_i$ transients in control and TRP5-transfected HEK cells in the presence of extracellular Ca^{2+}.** Cytosolic Ca^{2+} was measured in fura-2-loaded control HEK293 cells (*A*) or HEK293 cells transfected with TRP5 plus CD8 (*B*). The cells were treated with 100 μM ATP in the presence of 2 mM extracellular Ca^{2+}. The duration of exposure to Ca^{2+}-containing HBS and 100 μM ATP is indicated by the *filled* and *hatched bars*, respectively, above the graphs. *C*, dose-response relationships for maximum ATP-induced $[Ca^{2+}]_i$ rises ($\Delta[Ca^{2+}]_i$) in individual control HEK293 cells (*filled box*) or HEK293 cells transfected with TRP5 plus CD8 cDNAs (*filled circle*) in the presence of 2 mM extracellular Ca^{2+}, and in TRP5-transfected cells in the absence of extracellular Ca^{2+} (*open circle*). Data points are the means ± S.E. $[Ca^{2+}]_i$ (*A* and *B*) or the means ± S.E. $\Delta[Ca^{2+}]_i$ (*C*) in 30–41 control HEK cells or 14–20 TRP5-transfected cells.

cytoplasmic side, like other TRP subtypes (21–25, 42, 43). Domains that form coiled-coil structure were predicted on each side of the hydrophobic core (Fig. 1*A*) (44). Potential cAMP- and cGMP-dependent protein kinase phosphorylation sites Ser^{122} and Thr^{167} are assigned to the putative cytoplasmic regions. Fig. 1*C* depicts the phylogenetic tree of the TRP family constructed by the neighbor-joining method (45), based on the sequence alignment carried out by the Clustalw program (46). Sequence identity/similarity between TRP5 and bCCE (25), a bovine counterpart of TRP4 (24), was relatively high (67/79%), compared with identities/similarities between TRP5 and other TRP homologues (36–46/57–66%). Homology of TRP5 with TRP homologues is localized in the N-terminal region and the hydrophobic core (data not shown).

Tissue Distribution of TRP5—RNA preparations from different mouse tissues were subjected to Northern blot analysis using TRP5 cDNA as a specific probe (Fig. 2*A*). TRP5 mRNA was exclusively detected in the mouse central nervous system. An intense TRP5 signal with size of ~8.5 kb was present in the forebrain region (olfactory bulb, cerebrum, and midbrain) and a relatively weak signal was detected in the hindbrain region (cerebellum and medulla-pons). This contrasts with the predominant localization of TRP3 and TRP4 in the forebrain region and hindbrain region, respectively (47). To detect trace levels of TRP5 RNA expression in the tissues other than the brain, a pair of primers was designed to amplify cDNA sequences within the TRP5 cDNA probe used in the Northern analysis (Fig. 2*B*). RT-PCR amplification for 40 cycles, which is beyond the exponential phase of amplification, and subsequent Southern blot hybridization using a TRP5-specific oligonucleotide probe, disclosed TRP5 expression not only in the brain regions, but also in liver, kidney, testis, and uterus (48). In addition to the main hybridizable PCR product of ~330 base pairs, which corresponds to the expected size, a second hybridizable product of ~250 base pairs was detected in the hindbrain region, liver, kidney, testis, and uterus, but not in the forebrain.

Functional Characterization of TRP5: Cytosolic Ca^{2+} Measurements—HEK293 cells are capable of serving as an excellent expression system for studying functional properties of TRP5 as a receptor-activated Ca^{2+} channel, inasmuch as they have been known to endogenously express the P_2 purinoceptor coupled to activation of G_q protein and phospholipase C (49). HEK cells were also reported for the absence of endogenous TRP5 expression (48). TRP5, together with a marker protein CD8, was transiently expressed in HEK cells, and intracellular Ca^{2+} concentration was monitored in transfectants and nontransfected control HEK cells using fura-2 as an indicator. In the presence of 2 mM extracellular Ca^{2+}, application of 100 μM ATP to control cells induced a rapid rise in $[Ca^{2+}]_i$ that peaked within 30 s and gradually decreased to the resting level within 300 s (Fig. 3*A*). This transient rise in $[Ca^{2+}]_i$ was presumed to be mainly due to release from the intracellular Ca^{2+} store, because omission of extracellular Ca^{2+} little affected on the peak level (Fig. 4*A*), whereas the decay phase was accelerated in the absence of extracellular Ca^{2+}. When 100 μM ATP was applied to TRP5-transfected, CD8-positive cells in the presence of extracellular Ca^{2+}, the peak $[Ca^{2+}]_i$ level greatly increased (Fig. 3*B*). In TRP5-expressing cells, Ca^{2+} influx across the plasma membrane was likely to be a major cause of the $[Ca^{2+}]_i$

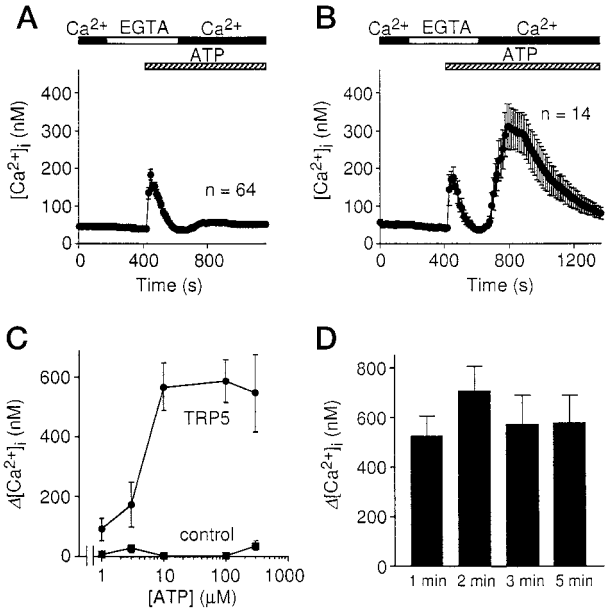

FIG. 4. **Separation of ATP-induced $[Ca^{2+}]_i$ transients due to Ca^{2+} release from internal stores and Ca^{2+} influx in TRP5-transfected HEK cells.** Cytosolic Ca^{2+} was measured in fura-2-loaded control HEK293 cells (*A*) or HEK293 cells transfected with TRP5 plus CD8 (*B*). In *A* and *B*, the perfusion solution was first changed to Ca^{2+}-free HBS containing 0.5 mM EGTA, and 100 μM ATP was applied to the cells in the absence of extracellular Ca^{2+}. Three min after the application of ATP, 2 mM Ca^{2+} was further added to the extracellular solution. The duration of exposure to Ca^{2+}-containing HBS, Ca^{2+}-free HBS, and 100 μM ATP is indicated by the *filled*, *open*, and *hatched bars*, respectively, above the graphs. *C*, concentration dependence of maximum $[Ca^{2+}]_i$ rises ($\Delta[Ca^{2+}]_i$) induced by the addition of 2 mM extracellular Ca^{2+} 3 min after the addition of ATP in individual control HEK293 cells (*filled box*) and HEK293 cells transfected with TRP5 plus CD8 (*filled circle*). *D*, $\Delta[Ca^{2+}]_i$ in TRP5-transfected cells are shown for various time intervals between the initiation of ATP (100 μM) application and the addition of 2 mM extracellular Ca^{2+}. Small $\Delta[Ca^{2+}]_i$ for 1 min resulted from $[Ca^{2+}]_i$, which was not yet reduced to the basal level before the addition of extracellular Ca^{2+}. Data points and columns are the means ± S.E. $[Ca^{2+}]_i$ or the means ± S.E. $\Delta[Ca^{2+}]_i$ in 29–64 control HEK cells or 14–16 TRP5-transfected cells.

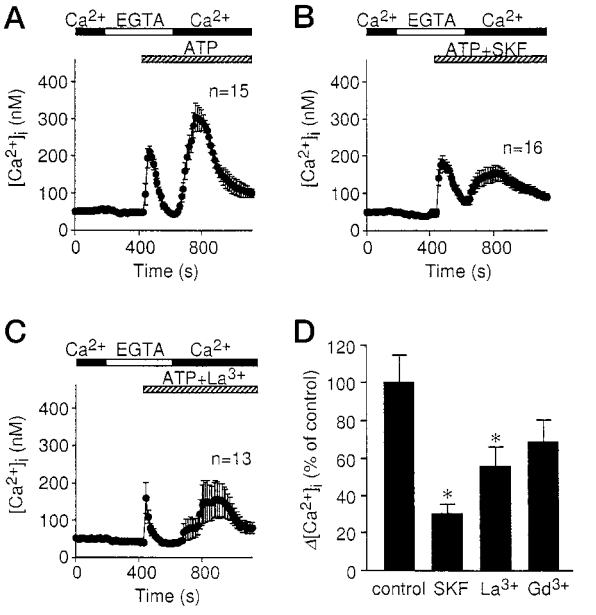

FIG. 5. **Pharmacological properties of ATP-induced Ca^{2+} influx in TRP5-transfected HEK cells.** Cytosolic Ca^{2+} was measured in fura-2-loaded TRP5-transfected cells. The perfusion solution was changed to Ca^{2+}-free HBS, and 100 μM ATP alone (*A* and *D*), with 25 μM SK&F96365 (*B* and *D*), with 100 μM $LaCl_3$ (*C* and *D*), or with 100 μM $GdCl_3$ (*D*) was applied to the cells in the absence of extracellular Ca^{2+}, which was followed by the addition of 2 mM extracellular Ca^{2+}. The duration of exposure to Ca^{2+}-containing HBS, Ca^{2+}-free HBS, and 100 μM ATP alone or plus one of the drugs is indicated by the *filled*, *open*, and *hatched bars*, respectively, above the graphs. *D*, effects of 25 μM SK&F96365, 100 μM $LaCl_3$, and 100 μM $GdCl_3$ on the amplitude of maximum $[Ca^{2+}]_i$ rises ($\Delta[Ca^{2+}]_i$) induced by the addition of 2 mM extracellular Ca^{2+} 3 min after the addition of ATP in individual TRP5-transfected cells. For the experiments using lanthanides and their control experiments, KH_2PO_4 was omitted from HBS. The data shown in *A* are from the experiments using the phosphate-containing solution. S.E. from the experiments using the phosphate-free external solutions is shown for control $\Delta[Ca^{2+}]_i$ shown in *D*. Data points and columns are the means ± S.E. $[Ca^{2+}]_i$ or the means ± S.E. $\Delta[Ca^{2+}]_i$ in 13–21 TRP5-transfected cells. Bonferroni's *t* test following analysis of variance was employed to determine the statistical significance of differences. *, $p < 0.05$, compared with the control.

rise, because the amplitude of $[Ca^{2+}]_i$ rise was much smaller in the absence of extracellular Ca^{2+} than that in the presence of extracellular Ca^{2+} at ATP concentrations above 1 μM (Fig. 3*C*), and remained almost the same as that of $[Ca^{2+}]_i$ transient evoked in control cells in the absence of extracellular Ca^{2+} (Fig. 4, *A* and *B*). $[Ca^{2+}]_i$ rise evoked by ATP in TRP5-expressing cells in the presence and absence of extracellular Ca^{2+}, and in control cells in the presence of extracellular Ca^{2+} increased in a similar dose-dependent manner (Fig. 3*C*).

To separate contribution to $[Ca^{2+}]_i$ rise of Ca^{2+} influx from that of Ca^{2+} release, ATP was first applied in the absence of extracellular Ca^{2+}, and 2 mM Ca^{2+} was then added to the extracellular solution when $[Ca^{2+}]_i$ returned to the resting level (3 min after addition of ATP). Addition of Ca^{2+} to the extracellular solution only slightly raised $[Ca^{2+}]_i$ above the resting level in control cells (Fig. 4, *A* and *C*), whereas in TRP5-transfected cells, it elicited dramatic $[Ca^{2+}]_i$ transients (Fig. 4, *B* and *C*), which reached maximum in the presence of ATP ≥ 10 μM (Fig. 4*C*). The second $[Ca^{2+}]_i$ rise evoked by extracellular Ca^{2+} did not seem to correlate with the preceding first $[Ca^{2+}]_i$ rise caused by ATP-dependent Ca^{2+} release from the intracellular Ca^{2+} store. The second $[Ca^{2+}]_i$ rise was 613 ± 77 (mean ± S.E.) nM for the TRP5-expressing cells that showed the first rise staying below 10 nM ($n = 16$), and was not significantly different from that (452 ± 40 nM) observed in the cells where the first rise was above 10 nM ($n = 48$). The time lag between start of ATP stimulation and addition of extracellular Ca^{2+} did not significantly affect amplitude of $[Ca^{2+}]_i$ rise up to 5 min (Fig. 4*D*). Interestingly, after 3 min of stimulation by ATP in Ca^{2+}-free solution, thapsigargin induced intact $[Ca^{2+}]_i$ rises in untransfected cells (102 ± 4 nM, $n = 53$), as compared with control cells without ATP stimulation (113 ± 5 nM, $n = 51$) (see below). Furthermore, after initial application of ATP for 3 min and subsequent omission of ATP up to 5 min in Ca^{2+}-free solution, untransfected cells did not show significant $[Ca^{2+}]_i$ rise induced by the second application of ATP ($n = 38$). These results suggest that ATP receptors are rapidly desensitized by incubating with 100 μM ATP, and thereby internal stores are replenished with Ca^{2+} within 3 min. Without ATP, $[Ca^{2+}]_i$ rise was not observed in TRP5-transfected cells that were immersed in the Ca^{2+}-containing solution after preincubation in the Ca^{2+}-free solution for up to 7 min (data not shown).

Lanthanides La^{3+} and Gd^{3+} were reported to block currents induced by recombinant expression of *Drosophila* TRP, TRPL, human TRP1, TRP3 (23, 24, 50), and native Ca^{2+} channels (51–53) and I_{CRAC} (54). The imidazol derivative, SK&F96365, inhibits various types of ion channels including receptor-activated channels (55, 56). In Fig. 5, 100 μM ATP was added alone (Fig. 5*A*) or together with one of the agents (25 μM SK&F96365 (Fig. 5*B*) or 100 μM La^{3+} (Fig. 5*C*)) to the Ca^{2+}-free extracellular solution, and 2 mM Ca^{2+} was added 3 min later. As shown in Fig. 5 (*B–D*), 25 μM SK&F96365 and 100 μM La^{3+} signifi-

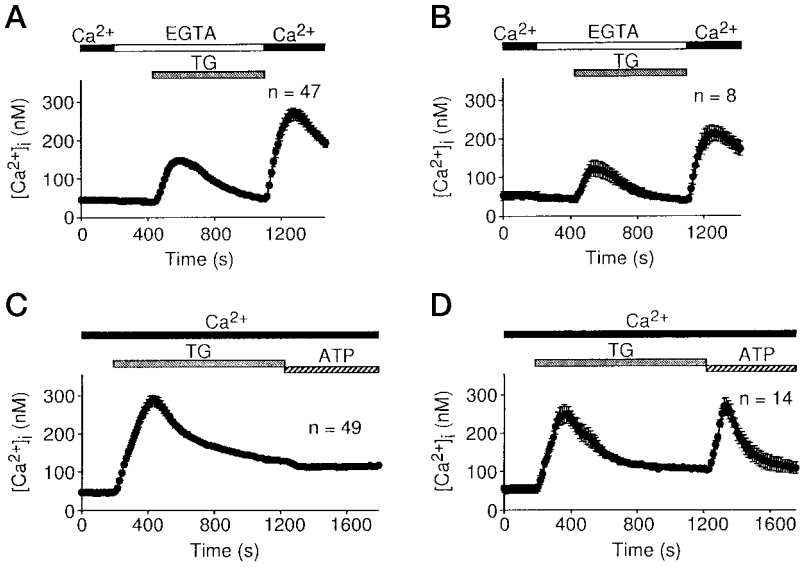

FIG. 6. **Thapsigargin-induced $[Ca^{2+}]_i$ transients and ATP-induced $[Ca^{2+}]_i$ changes after store depletion in control and TRP5-transfected HEK cells.** Cytosolic Ca^{2+} was measured in fura-2-loaded control HEK293 cells (*A* and *C*) or HEK293 cells transfected with TRP5 plus CD8 (*B* and *D*). In *A* and *B*, the perfusion solution was changed to Ca^{2+}-free HBS containing 0.5 mM EGTA, and 2 μM thapsigargin (*TG*) was applied to the cells in the absence of extracellular Ca^{2+}, which was followed by the addition of 2 mM extracellular Ca^{2+}. In *C* and *D*, the cells were treated with 2 μM thapsigargin in the presence of extracellular Ca^{2+}, then thapsigargin was replaced with 100 μM ATP. The duration of exposure to Ca^{2+}-containing HBS, Ca^{2+}-free HBS, 100 μM ATP, and 2 μM thapsigargin is indicated by the *filled*, *open*, *hatched*, and *shaded* bars, respectively, above the graphs. Data points are the means ± S.E. $[Ca^{2+}]_i$ in the indicated number of cells.

cantly suppressed the second $[Ca^{2+}]_i$ increase due to Ca^{2+} influx. However, compared with the two agents, the effect of 100 μM Gd^{3+} on the amplitude of the second $[Ca^{2+}]_i$ rise was not as significant (Fig. 5*D*). These results indicate that ATP-induced Ca^{2+} influx in TRP5-transfected cells is sensitive to blockade by SK&F96365 and La^{3+} (Fig. 5*D*).

To examine whether the $[Ca^{2+}]_i$ transient due to TRP5-mediated Ca^{2+} influx is activated by depletion of the intracellular Ca^{2+} store induced by IP_3-dependent Ca^{2+} release via phospholipase C stimulation, we used, instead of ATP, the specific inhibitor of sarcoplasmic and endoplasmic reticulum ATPases, thapsigargin (57). As the cells were perfused with Ca^{2+}-free solution containing 2 μM thapsigargin, $[Ca^{2+}]_i$ was transiently increased and thereafter reduced to the basal level (Fig. 6, *A* and *B*). Subsequent addition of Ca^{2+} (2 mM) to the extracellular solution transiently increased $[Ca^{2+}]_i$ in TRP5-transfected cells (Fig. 6*B*) to levels similar to those in control cells (Fig. 6*A*), indicating that CCE is not potentiated by expression of TRP5. This observation suggests that TRP5 is not activated by store depletion.

We further tested whether ATP is capable of activating Ca^{2+} influx in the TRP5-expressing cells where thapsigargin-induced Ca^{2+} influx is already activated. When cells were perfused with the solution containing 2 mM Ca^{2+} and 2 μM thapsigargin, transient $[Ca^{2+}]_i$ increase developed similarly in the control and transfected cells, decreasing within 1000 s after addition of thapsigargin to stationary levels that stayed slightly above the initial basal levels (Fig. 6, *C* and *D*). Replacement of thapsigargin with 100 μM ATP transiently increased $[Ca^{2+}]_i$ without any latency in TRP5-transfected cells (Fig. 6*D*), whereas it slightly decreased $[Ca^{2+}]_i$ in control cells (Fig. 6*C*). The results overall indicate that ATP activates Ca^{2+} influx by a trigger different from depletion of the Ca^{2+} store.

Functional Characterization of TRP5: Electrophysiological Measurements—To directly demonstrate that TRP5 is responsible for Ca^{2+} influx activated by ATP in HEK cells, ionic currents triggered by ATP stimulation in TRP5-transfected cells were characterized in comparison with those in control nontransfected HEK cells, using whole-cell mode of patch-clamp. When 200 nM free Ca^{2+} was present in the patch pipette, and ATP was added to the $0Ca^{2+}$ external solution, 16 out of 18 CD8-positive, TRP5-transfected HEK cells showed inward currents accompanied with an increase in the amplitude of current fluctuation (Fig. 7*B*). Rapid exchange of the $0Ca^{2+}$ external solution with the $10Ca^{2+}$ external solution

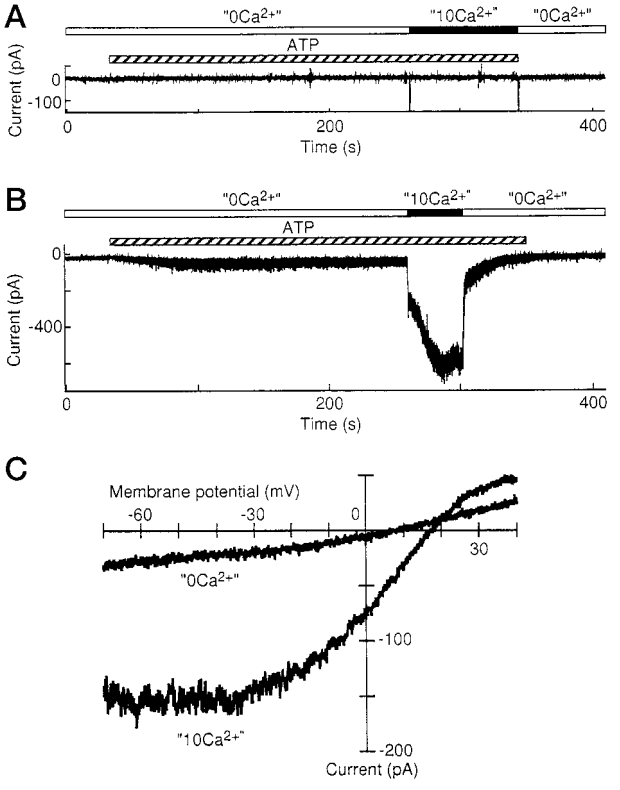

FIG. 7. **Electrophysiological characterization of the TRP5 channel.** In *A*, shown is a time course of ionic current recorded from a control HEK293 cell at a holding potential of −50 mV. During application of ATP (indicated by the *hatched bar* above the current) to the control HEK293 cell, the external solutions were changed from the $0Ca^{2+}$ solution (*open bar*) to the $10Ca^{2+}$ solution (*filled bar*). Finally, ATP was washed out with the $0Ca^{2+}$ solution. In *B*, a time course of ionic current recorded from a HEK293 cell transfected with TRP5 plus CD8 is shown. In *C*, current-voltage relationships of the TRP5 channel are shown. Currents were evoked by 1.5-s negative voltage ramps from 40 to −70 mV. Five consecutive ramps were applied every 5 s in the $0Ca^{2+}$ solution or the $10Ca^{2+}$ solution with 100 μM ATP. The averaged currents were drawn. The currents shown in *B* and *C* were recorded from different TRP5-transfected cells.

induced a rapid development of large inward currents, followed by a gradual increase of inward currents in 7 out of the 16 cells (Fig. 7*B*). The remaining nine cells did not show further increase of currents by the solution change. The augmentation of

the inward current was abolished quickly upon the removal of Ca^{2+}, although the fluctuation of currents remained until ATP was washed out. In the control cells ($n = 7$), 100 μM ATP did not induce significant ionic currents regardless of the presence of 10 mM Ca^{2+} in extracellular solution (Fig. 7*A*). When Ca^{2+} concentration in pipette solution was reduced to 50 nM, similar proportion of the CD8-positive, TRP5-transfected cells (11 out of 12 cells) showed responsiveness to ATP. However, usage of 10 nM free Ca^{2+} intrapipette solution resulted in a slightly reduced number of the CD8-positive, TRP5-transfected HEK cells responsive to ATP, inducing inward currents in six out of nine cells. The CD8-positive, TRP5-transfected HEK cells measured using the EGTA-containing, Ca^{2+}-free pipette solution were not responsive to ATP ($n = 5$).

Current-voltage relationship of ionic current triggered by ATP in TRP5-expressing cells was examined using negative voltage ramps from 40 to −70 mV for 1.5 s. Five consecutive voltage ramps were applied. The averages of current traces generated by five consecutive ramps every 5 s in the $0Ca^{2+}$ external solution and the $10Ca^{2+}$ external solution with 100 μM ATP were drawn in Fig. 7*C*. The current-voltage relationship recorded in $10Ca^{2+}$ was nonlinear, showing a significant inward current at physiological potentials. Permeability ratios among Na^+, Cs^+, and Ca^{2+} were estimated on the basis of the Goldman-Hodgkin-Katz equation using the reversal potentials in Fig. 7*C*. On the assumption that activity coefficients are 0.3 for Ca^{2+} and 0.75 for both Na^+ and Cs^+, the reversal potentials of 8 mV in the $0Ca^{2+}$ external solution and 17 mV in the $10Ca^{2+}$ solution lead to permeability ratios $P_{Ca}:P_{Na}:P_{Cs}$ = 14.3:1.5:1.

DISCUSSION

Activation Mechanism of TRP5 Essential for Receptor-activated Ca^{2+} Influx—In the present investigation, we have cloned and functionally characterized the mouse TRP homologue, designated as TRP5, predominantly expressed in the brain. Recombinant expression of the TRP5 cDNA in HEK cells potentiated transient increases in $[Ca^{2+}]_i$ evoked by ATP in the presence of extracellular Ca^{2+} (Fig. 3, *A* and *B*). When Ca^{2+} was added to the extracellular solution after preincubating the cells in the Ca^{2+}-free solution under constant ATP stimulation, potentiation of transient $[Ca^{2+}]_i$ rise induced by TRP5 expression became more prominent (Fig. 4, *A* and *B*). In this experiment, the second $[Ca^{2+}]_i$ rise due to Ca^{2+} influx showed no significant correlation with the first $[Ca^{2+}]_i$ rise due to Ca^{2+} release from IP_3-sensitive internal stores in the absence of extracellular Ca^{2+}. In an extreme case, $[Ca^{2+}]_i$ rise through Ca^{2+} influx was induced in a TRP5-expressing cell where Ca^{2+} release was hardly detectable. When thapsigargin was substituted for ATP to deplete the internal Ca^{2+} store by inhibiting ER Ca^{2+}-ATPases, the second $[Ca^{2+}]_i$ rise due to CCE was not potentiated by TRP5 expression (Fig. 6, *A* and *B*). These results indicate that TRP5 is responsible for Ca^{2+} influx activated by ATP via mechanisms other than Ca^{2+} depletion from the internal Ca^{2+} store.

The independence of TRP5-activating cascades from depletion of the internal Ca^{2+} stores is confirmed by additional lines of experimental evidence. In the presence of extracellular Ca^{2+}, after the thapsigargin-induced $[Ca^{2+}]_i$ transient decayed to a plateau level, another $[Ca^{2+}]_i$ rise was induced in TRP5-expressing cells by ATP (Fig. 6*D*), which did not induce $[Ca^{2+}]_i$ transients and even elicited slight decreases of $[Ca^{2+}]_i$ in control cells (Fig. 6*C*). The lack of ATP-induced Ca^{2+} release from ER in control cells after thapsigargin treatment (Fig. 6*C*) indicates that the ATP-sensitive stores are included in the thapsigargin-sensitive stores, excluding the possibility that TRP5 is activated via depletion of the ATP-sensitive stores independent of the thapsigargin-sensitive stores. It is also unlikely from this finding that TRP5 activation is directly coupled with the Ca^{2+}-releasing process involving the IP_3 receptors. Furthermore, our results indicate that after 3 min of stimulation by ATP in Ca^{2+}-free solution, TRP5 channels are still activable (Fig. 4*B*), but endogenous receptor-activated channels including CCE channels, whose activation by thapsigargin is clearly seen in Fig. 6*A*, are dormant in HEK cells (Fig. 4*A*). This is presumably due to differences between the TRP5 channel and endogenous channels in susceptibility to effects of ATP receptor desensitization. Desensitization of ATP receptors within 3 min is suggested from our experimental observation that in Ca^{2+}-free solution, $[Ca^{2+}]_i$ transient was not any more induced by ATP after initial application of ATP for 3 min and subsequent washing out of ATP for 5 min. Rapid desensitization of ATP receptors, compared with other types of receptors, was also reported by other groups (49). After a 3-min application of ATP in Ca^{2+}-free solution, $[Ca^{2+}]_i$ rise induced by subsequent application of thapsigargin was intact, suggesting that internal stores were rapidly replenished with Ca^{2+}. Thus, after desensitization of ATP receptors and replenishment of Ca^{2+} stores, activation signals for TRP5 channel still persist, whereas the activation trigger for CCE is already abolished.

From our experiments, some insights can be gained into the activation mechanism for TRP5. Present data imply an important role of Ca^{2+} in activation of TRP5. Whole-cell inward currents in ATP-stimulated, TRP5-transfected cells measured using the pipette solution containing free Ca^{2+} exhibited rapid and dramatic increases upon addition of Ca^{2+} to the extracellular solution (Fig. 7*B*), whereas those that were measured using the EGTA-containing, Ca^{2+}-free pipette solution were not responsive to ATP. $[Ca^{2+}]_i$ could be lowered to 10 nM, which is considerably lower than physiological $[Ca^{2+}]_i$, to elicit TRP5 current in HEK cells, whereas higher percentage of the TRP5 current-positive cells was obtained when $[Ca^{2+}]_i$ was elevated to 50 nM and 200 nM. This observation suggests that TRP5 is activable in the physiological range of $[Ca^{2+}]_i$ even at basal levels. Ca^{2+} may act through Ca^{2+}-binding proteins such as calmodulin and Ca^{2+}-dependent enzymes, although it is yet preliminary to make any conclusion with regard to the Ca^{2+} effect.

In thapsigargin-treated, TRP5-expressing cells, ATP primed the activity of TRP5 presumably not through $[Ca^{2+}]_i$ elevation (Fig. 6*D*), given that the action of ATP on $[Ca^{2+}]_i$ was toward decrease from slightly elevated levels in thapsigargin-treated control cells (Fig. 6*C*). This excludes the possibility that Ca^{2+} is a sole activation trigger for TRP5, strongly suggesting involvement of other factors in TRP5 activation. It is possible that slight decrease from the elevated level (in the presence of thapsigargin) optimizes $[Ca^{2+}]_i$ in the range that activates but does not inactivate TRP5. Activation of G_q protein, phospholipase C-β, and protein kinase C, and production of phosphoinositide metabolites such as IP_3 and IP_4, which are all triggered by stimulation of ATP receptors, should be considered as candidate activators of TRP5.

The results obtained are also indicative of a role of Ca^{2+} as a negative regulator for TRP5. In the presence of extracellular Ca^{2+}, $[Ca^{2+}]_i$ transients induced by ATP stimulation decreased almost to the basal level (Fig. 3*B*) at the time when the second $[Ca^{2+}]_i$ rise induced by Ca^{2+} addition with time lag of 3 min after ATP stimulation reached peak (Fig. 4*B*). Negative regulatory action of Ca^{2+} has been reported for *Drosophila* TRP, TRPL (30), and CCE in *Xenopus* oocytes (58).

Human TRP3 has been reported to form a nonselective cation channel that is not sensitive to Ca^{2+} store depletion (59, 60). Specifically, Zitt *et al.* (59) have shown that Ca^{2+} neither

act alone or act together with calmodulin directly on the TRP3 protein to activate the channel. Since the submission of the first version of this manuscript, we have learned that mouse TRP6 encodes a nonselective cation channel stimulated by the muscarinic M5 receptor, but not by intracellular store depletion (61). It is therefore possible that the Ca^{2+}-selective TRP5 channels are activated via common activation mechanisms that operate in opening the TRP3 channel and/or the TRP6 channel.

Functional Correlation of TRP Homologues and Native Receptor-activated Ca^{2+} Channels—Functional correspondence between cloned TRP homologues and Ca^{2+} channels responsible for receptor-activated Ca^{2+} influx, including CCE, in native preparations is still very controversial. Ca^{2+} selectivity in permeation has been one of the important criteria in correlating recombinant TRP homologues with native Ca^{2+} channels (32). Our whole-cell current measurements using patch pipettes filled with the solution containing 200 nM free Ca^{2+} demonstrated that rapid exchange of the external $0Ca^{2+}$ solution with the $10Ca^{2+}$ solution elicited instantaneous and dramatic increases of inward TRP5 currents (Fig. 7*B*), which reversed at positive potentials (Fig. 7*C*). This, together with the permeability ratios (P_{Ca}:P_{Na}:P_{Cs} = 14.3:1.5:1) calculated from the reversal potentials, indicates that TRP5 is selective for Ca^{2+} over monovalent cations. Of the other recombinantly expressed TRP homologues, *Drosophila* TRP and mammalian TRP4 were demonstrated for Ca^{2+} selectivity (25, 26, 30), whereas *Drosophila* TRPL and mammalian TRP1 and TRP3 were rather classified as nonselective cation channels (23, 27, 30, 59, 62). In the native systems, the TRP and TRPL components of light-activated current isolated through usage of *trpl* and *trp* mutant photoreceptors showed ion selectivity comparable with those of the recombinant TRP and TRPL (19, 63). Among the receptor-activated Ca^{2+} channels in vertebrate cells, known for diversity in ion permeation properties (3), some display ion selectivity that may correspond well to TRP homologues. However, establishing functional correlation of TRP with native receptor-activated Ca^{2+} channels becomes considerably unsuccessful by introduction of activation trigger as a second distinguishing criterion. Although I_{CRAC} is similar to TRP5 in selectivity for Ca^{2+} over Na^+, Ba^{2+}, and Mn^{2+} (64),[2] depletion of the intracellular Ca^{2+} store activates I_{CRAC} and the nonselective cation channels TRP1 (23) and TRP3 (62), but not Ca^{2+}-selective TRP5. In contrast to TRP5, IP_4 and Ca^{2+}-sensitive channels in endothelial cells are highly permeable not only to Ca^{2+}, but also to other divalent cations such as Ba^{2+} and Mn^{2+} (16). It has been also reported that Ba^{2+} or monovalent cations are as permeant as Ca^{2+} in other receptor-activated Ca^{2+} channels triggered by second messengers such as IP_3 or by activation of G-proteins (3). Thus, each vertebrate TRP homologue expressed in heterologous systems does not really correspond to the native receptor-activated Ca^{2+} channels in both the two functional criteria: activation trigger and Ca^{2+} selectivity.

Heteromultimer formation by multiple TRP isoforms (30) may be necessary to elicit native type receptor-activated Ca^{2+} entry. In our expression studies of TRP5, there was no clear functional indication for presence of heterogeneous populations of heteromultimer and homomultimer, although Garcia and Schilling (48) have shown expression of TRP1, TRP3, TRP4, and TRP6 mRNAs in HEK 293 cells. This may derive from the usage of ATP receptor stimulation in activating Ca^{2+} entry, or low mRNA expression levels of endogenous TRP isoforms compared with the level of TRP5 overexpression. It would be necessary to characterize functional properties of neuronal receptor-activated Ca^{2+} channels at exact expression sites of individual TRP homologues determined by *in situ* hybridization (47, 65) and immunohistochemistry in native tissues, and to compare them with those of recombinant receptor-activated channels composed of appropriate TRP combinations.

Acknowledgments—We thank Drs. Brian Seed and Gary Yellen for the CD8 expression plasmid, Dr. Kouhei Sawada for the accessibility to $[Ca^{2+}]_i$ measurement systems, and Emiko Mori for expert technical assistance.

[2] T. Okada, S. Shimizu, M. Wakamori, A. Maeda, T. Kurosaki, N. Takada, K. Imoto, and Y. Mori, unpublished data.

REFERENCES

1. Tsien, R. W., and Tsien, R. Y. (1990) *Annu. Rev. Cell Biol.* **6,** 715–760
2. Clapham, D. E. (1995) *Cell* **80,** 259–268
3. Fasolato, C., Innocenti, B., and Pozzan, T. (1994) *Trends Pharmacol. Sci.* **15,** 77–83
4. Putney, J. W. (1990) *Cell Calcium* **11,** 611–624
5. Irvine, R. F. (1990) *FEBS Lett.* **263,** 5–9
6. Putney, J. W., Jr., and Bird, G. St. J. (1993) *Cell* **75,** 199–201
7. Partiseti, M., Le Deist, F., Hivroz, C., Fischer, A., Korn, H., and Choquet, D. (1994) *J. Biol. Chem.* **269,** 32327–32335
8. Serafini, A. T., Lewis, R. S., Clipstone, N. A., Bram, R. J., Fanger, C., Fiering, S., Herzenberg, L. A., and Crabtree, G. R. (1995) *Immunity* **3,** 239–250
9. Berridge, M. J. (1995) *Biochem. J.* **312,** 1–11
10. Randriamampita, C., and Tsien, R. Y. (1993) *Nature* **364,** 809–814
11. Parekh, A. B., Terlau, H., and Stühmer, W. (1993) *Nature* **364,** 814–818
12. Parekh, A. B., Fleig, A., and Penner, R. (1997) *Cell* **89,** 973–980
13. Kuno, M., and Gardner, P. (1987) *Nature* **326,** 301–304
14. Restrepo, D., Miyamoto, T., Bryant, B. P., and Teeter, J. H. (1990) *Science* **249,** 1166–1168
15. Mozhayeva, G. N., Naumov, A. P., and Kuryshev, Y. A. (1991) *J. Membr. Biol.* **124,** 113–126
16. Luckhoff, A., and Clapham, D. E. (1992) *Nature* **355,** 356–358
17. Fein, A., Payne, R., Corson, D. W., Berridge, M. J., and Irvine, R. F. (1984) *Nature* **311,** 157–160
18. Ranganathan, R., Malicki, D. M., and Zuker, C. S. (1995) *Annu. Rev. Neurosci.* **18,** 283–317
19. Niemeyer, B. A., Suzuki, E., Scott, K., Jalink, K., and Zuker, C. S. (1996) *Cell* **85,** 651–659
20. Petersen, C. C. H., Berridge, M. J., Borgese, M. F., and Bennett, D. L. (1995) *Biochem. J.* **311,** 41–44
21. Wes, P. D., Chevesich, J., Jeromin, A., Rosenberg, C., Stetten, G., and Montell, C. (1995) *Proc. Natl. Acad. Sci. U. S. A.* **92,** 9652–9656
22. Zhu, X., Chu, P. B., Peyton, M., and Birnbaumer, L. (1995) *FEBS Lett.* **373,** 193–198
23. Zitt, C., Zobel, A., Obukhov, A. G., Harteneck, C., Kalkbrenner, F., Lückhoff, A., and Schultz, G. (1996) *Neuron* **16,** 1189–1196
24. Zhu, X., Jiang, M., Peyton, M., Boulay, G., Hurst, R., Stefani, E., and Birnbaumer, L. (1996) *Cell* **85,** 661–671
25. Philipp, S., Cavalié, A., Freichel, M., Wissenbach, U., Zimmer, S., Trost, C., Marquart, A., Murakami, M., and Flockerzi, V. (1996) *EMBO J.* **15,** 6166–6171
26. Vaca, L., Sinkins, W. G., Hu, Y., Kunze, D. L., and Schilling, W. P. (1994) *Am. J. Physiol.* **267,** C1501–C1505
27. Hu, Y., and Schilling, W. P. (1995) *Biochem. J.* **305,** 605–611
28. Obukhov, A. G., Harteneck, C., Zobel, A., Harhammer, R., Kalkbrenner, F., Leopoldt, D., Lückhoff, A., Nürnberg, B., and Schultz, G. (1996) *EMBO J.* **15,** 5833–5838
29. Hardie, R. C., Reuss, H., Lansdell, S. J., and Millar, N. S. (1997) *Cell Calcium* **21,** 431–440
30. Xu, X.-Z. S., Li, H.-S., Guggino, W. B., and Montell, C. (1997) *Cell* **89,** 1155–1164
31. Preuß, K.-D., Nöller, J. K., Krause, E., Göbel, A., and Schulz, I. (1997) *Biochem. Biophys. Res. Commun.* **240,** 167–172
32. Clapham, D. E. (1996) *Neuron* **16,** 1069–1072
33. Acharya, J. K., Jalink, K., Hardy, R. W., Hartenstein, V., and Zuker, C. S. (1997) *Neuron* **13,** 881–887
34. Mori, Y., Friedrich, T., Kim, M.-S., Mikami, A., Nakai, J., Ruth, P., Bosse, E., Hofmann, F., Flockerzi, V., Furuichi, T., Mikoshiba, K., Imoto, K., Tanabe, T., and Numa, S. (1991) *Nature* **350,** 398–402
35. Jobling, S. A., and Gehrke, L. (1987) *Nature* **325,** 622–625
36. Kozak, M. (1986) *Cell* **44,** 283–292
37. Jurman, M. E., Boland, L. M., Liu, Y., and Yellen, G. (1994) *BioTechniques* **17,** 876–881
38. Hazama, A., and Okada, Y. (1990) *Pflügers Arch. Eur. J. Physiol.* **416,** 710–714
39. Ueda, S., and Okada, Y. (1989) *Biochim. Biophys. Acta* **1012,** 254–260
40. Hamill, O. P., Marty, A., Neher, E., Sakmann, B., and Sigworth, F. J. (1981) *Pflügers Arch. Eur. J. Physiol.* **391,** 85–100
41. Nakagawa, T., Shirasaki, T., Wakamori, M., Fukuda, A., and Akaike, N. (1990) *Neurosci. Res.* **8,** 114–123
42. Montell, C., and Rubin, G. M. (1989) *Neuron* **2,** 1313–1323
43. Phillips, A. M., Bull, A., and Kelly, L. E. (1992) *Neuron* **8,** 631–642
44. Lupas, A., Van Dyke, M., and Stock, J. (1991) *Science* **252,** 1162–1164
45. Saitou, N., and Nei, M. (1987) *Mol. Biol. Evol.* **4,** 406–425
46. Thompson, J. D., Higgins, D. G., and Gibson, T. J. (1994) *Nucleic Acids Res.* **22,** 4673–4680
47. Mori, Y., Takada, N., Okada, T., Wakamori, M., Imoto, K., Wanifuchi, H., Oka, H., Oba, A., Ikenaka, K., and Kurosaki, T. (1998) *NeuroReport* **9,** 507–515
48. Garcia, R. L., and Schilling, W. P. (1997) *Biochem. Biophys. Res. Commun.* **239,** 279–283

49. Bischof, G., Serwold, T. F., and Machen, T. E. (1997) *Cell Calcium* **21,** 135–142
50. Sinkins, W. G., Vaca, L., Hu, Y., Kunze, D. L., and Schilling, W. P. (1996) *J. Biol. Chem.* **271,** 2955–2960
51. Boland, L. M., Brown, T. A., and Dinglendine, R. (1991) *Brain Res.* **563,** 142–150
52. Lacampagne, A., Gannier, F., Argibay, J., Garnier, D., and Le Guennec, J. Y. (1994) *Biochim. Biophys. Acta* **1191,** 205–208
53. Chang, W., Chen, T. H., Gardner, P., and Shoback, D. (1995) *Am. J. Physiol.* **269,** E864–E877
54. Hoth, M, and Penner, R. (1993) *J. Physiol.* **465,** 359–386
55. Clementi, E., and Meldolesi, J. (1996) *Cell Calcium* **19,** 269–279
56. Waldron, R. T., Short, A. D., and Gill, D. L. (1997) *J. Biol. Chem.* **272,** 6440–6447
57. Inesi, G., and Sagara, Y. (1994) *J. Membr. Biol.* **141,** 1–6
58. Petersen, C. C. H., and Berridge, M. J. (1994) *J. Biol. Chem.* **269,** 32246–32253
59. Zitt, C., Obukhov, A. G., Strübing, C., Zobel, A., Kalkbrenner, F., Lückhoff, A., and Schultz, G. (1997) *J. Cell Biol.* **138,** 1333–1341
60. Zhu, X., Jiang, M., Birnbaumer, L. (1998) *J. Biol. Chem.* **273,** 133–142
61. Boulay, G., Zhu, X., Peyton, M., Jiang, M., Hurst, R., Stefani, E., and Birnbaumer, L. (1997) *J. Biol. Chem.* **272,** 29672–29680
62. Birnbaumer, L., Zhu, X., Jiang, M., Boulay, G., Peyton, M., Vannier, B., Brown, D., Platano, D., Sadeghi, H., Stefani, E., and Birnbaumer, M. (1996) *Proc. Natl. Acad. Sci. U. S. A.* **93,** 15195–15202
63. Hardie, R. C., and Minke, B. (1992) *Neuron* **8,** 643–651
64. Hoth, M., and Penner, R. (1992) *Nature* **355,** 353–356
65. Funayama, M., Goto, K., and Kondo, H. (1996) *Mol. Brain Res.* **43,** 259–266
66. Kyte, J., and Doolittle, R. F. (1982) *J. Mol. Biol.* **157,** 105–132
67. Sulston, J., Du, Z., Thomas, K., Wilson, R., Hillier, L., Staden, R., Halloran, N., Green, P., Thierry-Mieg, J., Qiu, L., Dear, S., Coulson, A., Craxton, M., Durbin, R., Berks, M., Metzstein, M., Hawkins, T., Ainscough, R., and Waterston, R. (1992) *Nature* **356,** 37–41
68. Sakura, H., and Ashcroft, F. M. (1997) *Diabetologia* **40,** 528–532